# The Effect of Ni Content on Lateral Diffusion of Alloyed Au-Ni-AuGe Ohmic Contacts in GaAs-AlGaAs-InGaAs pHEMT Structures

Mike Powers, John Staroba, and Chien-Chia Cheng

Agilent Technologies, 1400 Fountaingrove Parkway, Santa Rosa, CA 95403, (707) 577-4022, mike.powers@agilent.com

**Keywords: GaAs-AlGaAs-InGaAs, pHEMT, Ohmic Contacts, Ni-AuGe, Ni Content, Ohmic Runout**

## Abstract

**Alloyed Ohmic contacts in GaAs-AlGaAs-InGaAs pHEMTs fabricated by sequential e-beam evaporation of Au-Ni-AuGe metallization layers can sporadically suffer from lateral diffusion anomalies, referred to here as “ohmic runout.” This investigation studied the influence of Au to Ge compositional ratio and Ni content on the alloyed ohmic runout behavior. It was found that the degree of ohmic runout is critically sensitive to the volume fraction of Ni in the metallization stack and that decreasing the Ni content mitigated ohmic runout without compromising the alloyed ohmic contact resistance.**

## INTRODUCTION

The quality of source and drain ohmic contacts in GaAs-AlGaAs-InGaAs pseudomorphic high electron mobility transistor (pHEMT) structures is critical to the performance and reliability of the devices. Since the introduction of the Ni-AuGe ohmic contact to GaAs by Braslau [1], it has become the most widely used for *n*-type contacts because low contact resistance can be achieved by controlled vertical diffusion of the contact metals during alloy into the active device channel. In this contact system, Au acts as a base metal and Ge acts as a dopant element, so that tunneling is the dominant transport mechanism. A number of researchers have reported on the phenomenon of lateral diffusion at the GaAs/AlGaAs interface for Ni-AuGe contacts [2-5]. In some reported cases, the lateral encroachment of the contact metal was significant enough (0.2 to 0.25 µm) to result in source-drain shorts in TLM measurement structures, due to the close spacing of the contacts [6]. Attempts to mitigate the effect of contact metal lateral diffusion by increasing the alloy temperature [7], transient thermal annealing [8], lowering the alloy temperature [9], utilization of a hypoeutectic AuGe composition [10], rapid thermal annealing [11] and various approaches that employ alternative ohmic contact metals have been met with limited success.

The phenomenon of ohmic runout (i.e. lateral diffusion, lateral excursion, lateral protrusion, or lateral encroachment) is not new; it is an issue that has beleaguered process engineers and researchers for decades. One team of investigators was led to conclude that “the observed lateral diffusion at the edge of the contacts produced an effective contact extension and should, therefore, be taken into account when designing and modeling submicron devices.” [2] Another paper concluded that “the contact structure provides a limit for minimum source-drain spacings and should also be considered from a device reliability standpoint.” [9]

Iliadis et al. [6] proposed a promising method for mitigation of ohmic runout where a low temperature (250° C) anneal with slow ramp-rate-to-peak temperature processing was employed. However, this approach was developed for relatively thin (300 Å total) epitaxial layers above the active channel in the substrate and is not applicable to cases where the epitaxial structure is much thicker (e.g. > 900 Å total), as is the case for this study.

## EXPERIMENTAL PROCEDURE

The ohmic contact metallization structures in this investigation were fabricated in Temescal FC-2800 e-beam evaporators by sequential deposition of Au (300 Å), Ge (400 Å), Au (600 Å), Ni (260 Å), Au (2000 Å) and Ti (200 Å) on top of the $n^+$ GaAs contact layer of an GaAs-AlGaAs-InGaAs pHEMT structure. The standard deposition process employed a three minute *in situ* ion mill sequence with a nominal etch rate of 8 Å/minute, corresponding to 24 Å of material removal. Following ohmic metal deposition and lift-off, an 800 Å $SiO_x$ cap was deposited using a Trikon Delta PECVD system. The ohmic contacts were then alloyed at 426° C for 30 seconds under a nitrogen gas blanket using a Solitec 820 alloy system.

SEM cross section micrographs of as-deposited and alloyed ohmic contact structures were generated using a Ziess Auriga 40 FIB-SEM. Plan view optical micrographs were produced using an Olympus MX61A Microscope Inspection Station. TEM specimens were prepared using the *in situ* FIB lift-out technique using an FEI Strata 400 FIB-SEM and imaged in an FEI Tecnai TF-20 TEM operated at 200 kV. X-ray spectra were acquired using an Oxford INCA EDS system.

In a first set of experiments, the relative Ge content in the ohmic contact stack was varied from 8 wt. % (hypoeutectic composition) to 20 wt. % (hypereutectic composition) in order to study the effect of the Au to Ge ratio on ohmic runout. The thickness of the Au and Ge layers below the Ni layer in the metallization layer stack was adjusted to produce five compositions corresponding to specific locations on the Au-Ge binary phase diagram; 92%Au-8%Ge, 89%Au-11%Ge, 88%Au-12%Ge (eutectic), 87%Au-13%Ge (control composition) and 80%Au-20%Ge. Two wafers at each of the five Au-Ge ratios were tested.

In a second set of experiments, the relative Ni volume fraction in the ohmic stack was varied from 0.154 - 0.246 to explore the effect of Ni content on ohmic runout. The thickness of the Ni layer in the layer stack was modified in order to generate five Ni to AuGe volume fractions; 0.154 (200 Å Ni), 0.176 (230 Å Ni), 0.200 (260 Å Ni – control thickness), 0.220 (290 Å Ni) and 0.246 (320 Å Ni). One wafer at each of the five Ni fractions was tested and the experiment was run three times in three different evaporation systems.

The contact resistance ($R_c$) of the alloyed ohmic contacts was characterized by TLM measurements [12] using test structures with contact spacings of 3, 6, 9 and 12 μm. Seventy sets of test structures were measured on each test wafer and the extrapolated $R_c$ values were averaged.

## RESULTS AND DISCUSSION

Figure 1 shows a FIB-SEM cross section of an as-deposited ohmic structure, while Figure 2 shows the ohmic structure after the alloy sequence. The Ni layer in the middle of the metallization stack of Figure 1 appears in gray contrast. The post alloy ohmic runout at the periphery of the contact in Figure 2 is significant and extends over 0.27 microns from the edge of the alloyed contact structure.

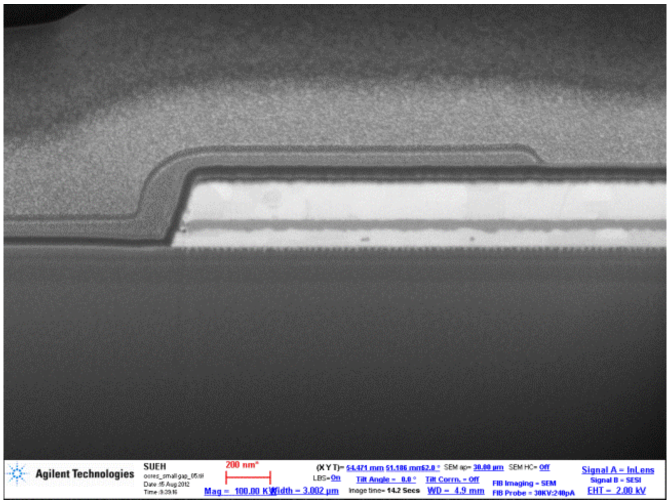

Figure 1. SEM micrograph of an as-deposited ohmic contact structure.

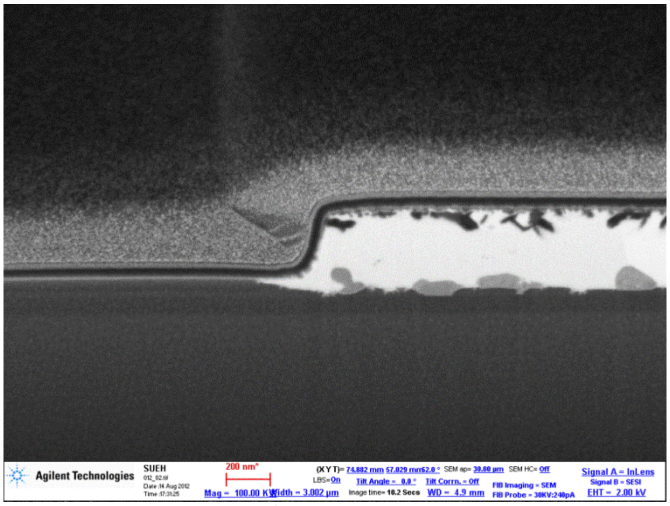

Figure 2. SEM micrograph of the alloyed contact showing ohmic runout.

Figure 3 shows an optical plan view micrograph at 500x magnification and a corresponding SEM cross section of an ohmic contact test structure from an alloyed test wafer with the eutectic composition of 88%Au-12%Ge. There is no evidence of ohmic runout in either image.

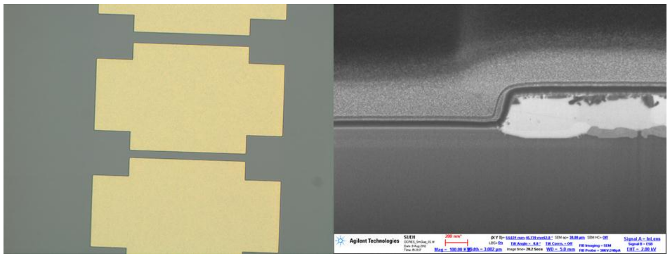

Figure 3. 500x optical (left) & SEM x-section (right) of an 88Au-12Ge OC.

By contrast, Figure 4 shows a 500x optical plan view micrograph and the corresponding SEM cross section of an alloyed ohmic contact with a hypereutectic composition of 80%Au-20%Ge. Pronounced ohmic runout is evident in both images. The lateral diffusion in the SEM cross section image extends almost a full micron from the edge of the structure.

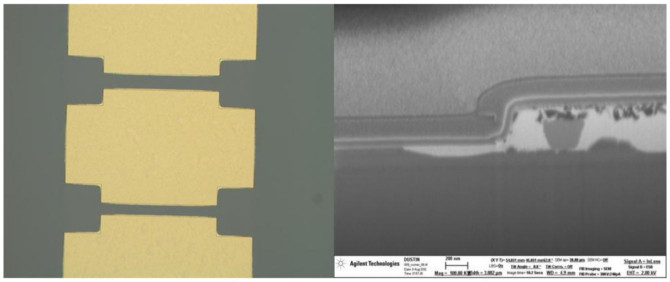

Figure 4. 500x optical (left) & SEM x-section (right) of an 80Au-20Ge OC.

It was found that the hypoeutectic compositions (8% and 11% Ge), the eutectic composition (88%Au-12%Ge) and a slightly hypereutectic composition (13% Ge) did not display any evidence of ohmic runout. By contrast, wafers with a hypereutectic composition of 80%Au-20%Ge consistently displayed moderate to severe ohmic runout after alloying with only modest vertical diffusion into the GaAs substrate.

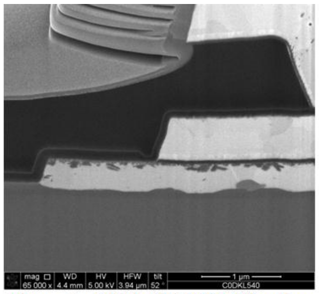

Figure 5a. SEM of 0.176 Ni fraction.

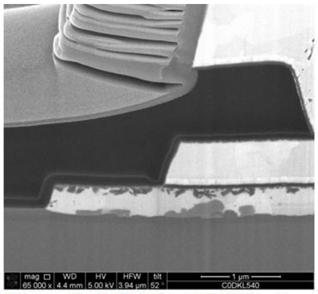

Figure 5b. SEM of 0.200 Ni fraction.

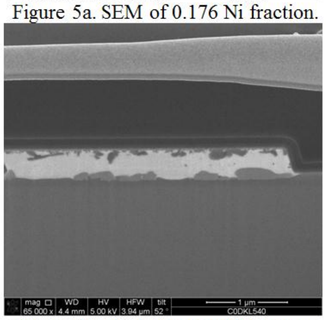

Figure 5c. SEM of 0.220 Ni fraction.

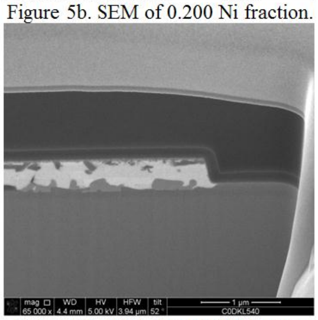

Figure 5d. SEM of 0.246 Ni fraction.

Figure 5a-5d shows a series of FIB-SEM cross sections, after alloy, where the Ni to AuGe volume fraction in the ohmic metallization stack was varied from 0.176 to 0.246. It is clear that the lower Ni volume fractions (0.176 and 0.200) which correspond respectively to 230 Å and 260 Å of Ni in the ohmic metallization stack show no evidence of ohmic runout. Conversely, the ohmic runout for the sample with a Ni volume fraction of 0.22 (290 Å Ni) in Figure 5c is modest, whereas the ohmic runout for the sample with a Ni volume fraction of 0.246 (320 Å Ni) in Figure 5d is more significant. This experiment was reproduced in three evaporation systems and in each test, the results were consistent in that the higher Ni content ohmic structures evidenced ohmic runout while the lower Ni content structures did not.

A notable aspect of the Ni content experiments is the associated contact resistance results. Table 1 shows the average $R_c$ values for each set of wafers with a particular Ni thickness. The average $R_c$ of 0.22 Ω-mm for the control wafer (260 Å Ni) is a typical value. Test wafers with moderate (290 Å Ni) and more pronounced (320 Å Ni) ohmic runout also displayed higher contact resistance compared to the control wafer. However, it is interesting to note that the test wafers with a Ni thickness less than the control returned discernibly lower average contact resistance.

TABLE 1
CONTACT RESISTANCE AS A FUNCTION OF NICKEL THICKNESS

| Ni Thk (Å) | Avg $R_c$ (Ω-mm) | Std Dev | Comment |
|---|---|---|---|
| 320 | 0.33 | 0.018 | |
| 290 | 0.32 | 0.044 | |
| 260 | 0.22 | 0.016 | Control |
| 230 | 0.19 | 0.004 | |
| 200 | 0.19 | 0.012 | |

Historically, the function of the Ni layer in the Ni-AuGe contact structure has variously been cited as a diffusion barrier [13], as an adhesion promoter [14], as a wetting agent [15], to decrease surface roughness and improve uniformity [16], as an aid to consumption of native oxides [17] and to improve thermal stability of the alloyed contact [18]. By now it is well established that Ni is an active participant in the interfacial reactions and the presence of Ni is important for optimum electrical performance of the alloyed ohmic contact by formation of a NiAsGe compound at the metal-semiconductor interface [19, 20].

The high angle annular dark field (HAADF) TEM image in Figure 6 shows an alloyed ohmic contact structure from a test wafer with a 320 Å thick Ni layer, which displays ohmic runout at the edge of the structure. The alloyed contact has penetrated into the InGaAs active channel layer. Table 2 lists the concentration of elements (in atomic %), determined with EDS, corresponding to the locations indicated in Figure 6. The EDS results indicate that the compounds formed at the interface consist of interspersed NiAsGe (e.g. locations 3, 4 and 6) and AuGa (location 14) grains, which is consistent with those reported in the literature for the Ni-AuGe contact system [19-21].

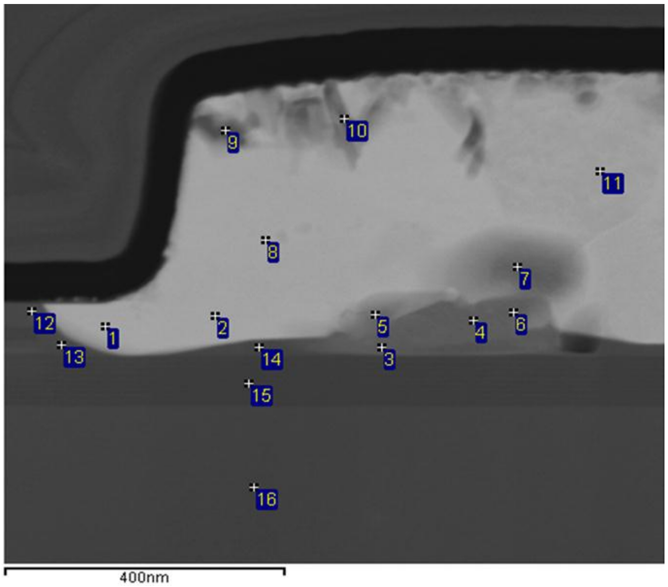

Figure 6. TEM micrograph of an alloyed OC structure with 320 Å Ni.

TABLE 2
% ELEMENTAL CONCENTRATIONS FOR LOCATIONS IN FIGURE 6

| Location | Ti | Ni | Ga | Ge | As | Au |
|---|---|---|---|---|---|---|
| 1 | - | - | 7.6 | - | - | 92.4 |
| 2 | - | - | 5.6 | - | - | 94.4 |
| 3 | - | 48.2 | - | 23.8 | 28.0 | - |
| 4 | - | 48.2 | - | 32.8 | 19.0 | - |
| 5 | - | 44.3 | - | 39.7 | 5.6 | 10.4 |
| 6 | - | 51.5 | - | 25.3 | 23.2 | - |
| 7 | - | 49.4 | - | 17.4 | 30.7 | 2.5 |
| 8 | - | - | 8.7 | - | - | 91.3 |
| 9 | 39.1 | 9.6 |  | 4.8 | 46.5 | - |
| 10 | 16.8 | 7.2 | 4.5 | - | 26.7 | 44.8 |
| 11 | - | - | 6.1 | - | - | 93.9 |
| 12 | - | - | 26.3 | 46.2 | 23.4 | 4.1 |
| 13 | - | - | 50.6 | - | 49.4 | - |
| 14 | - | - | 47.9 | - | 52.1 | - |
| 15 | - | - | 45.1 | - | 54.9 | - |
| 16 | - | - | 50.4 | - | 49.6 | - |

## CONCLUSIONS

The key result of this investigation is the critical sensitivity of ohmic runout on the Ni content in the ohmic metal stack. We have found that a higher volume fraction of Ni to Au-Ge (0.22 – 0.25) in the ohmic deposition layer stack exacerbates ohmic runout and increases contact resistance to unacceptable values, whereas a lower volume fraction of Ni (0.15 – 0.20) eliminates ohmic runout without compromising the contact resistance of the ohmic contact.

## REFERENCES

[1] N. Braslau, J.B. Gunn, and J.L. Staples, "Metal-Semiconductor contacts for GaAs bulk effect devices," *Solid-State Electron.*, Vol. 10, pp. 381-383, 1967.

[2] D.W. Langer, A. Ezis and A.K. Rai, "Structure and lateral diffusion of ohmic contacts in AlGaAs/GaAs high electron mobility transistors and GaAs devices," *J. Vac. Sci. Technol. B*, Vol. 5, No. 4, pp. 1030-1032, 1987.

[3] G.S. Marlow, M.B. Das and L. Tongson, "The characteristics of Au-Ge-based ohmic contacts to *n*-GaAs including the effects of aging," *Solid-State Electron.*, Vol. 26, pp. 259-266, 1983.

[4] M. Procop and B. Sandow, "Au-Ge based ohmic contacts on GaAs," *Phys. Status Solidi*, Vol. A 95, pp. K211-K215, 1986.

[5] A.A. Lakhani, R.C. Potter and D.M. Beyea, "Application of a resonant tunneling structure to demonstrate subsurface damage and surface migration on InGaAs during AuGe contact anneal," *Semicond. Sci. Technol. 3*, pp. 605-607, 1988.

[6] A.A. Iliadis, J.K. Zahurak, T. Neal and W.T. Masselink, "Lateral diffusion effects in AuGe based source-drain contacts to AlInAs/InGaAs/InP doped channel MODFETs," *J. Electron. Mater.*, Vol. 28, No. 8, pp. 944-948, 1999.

[7] M. Ogawa, "Alloying behavior of Ni/Au-Ge films on GaAs," *J. Appl. Phys.*, Vol. 51, No. 1, pp. 406-412, 1980.

[8] A.K. Rai, A. Ezis, R.J. Graham, R. Sharma and D.W. Langer, "Microstructural characterization of AlGaAs-GaAs modulation-doped field-effect transistor ohmic contacts formed by transient annealing," *J. Appl. Phys.*, Vol. 63, No. 9, pp. 4723-4727, 1987.

[9] A. Ezis, A.K. Rai and D.W. Langer, "Lateral protrusions of ohmic contacts to AlGaAs/GaAs MODFET material," *Electron. Lett.*, Vol. 23, p. 113, 1987.

[10] H. Goronkin, S. Tehrani, T. Remmel, P.L. Fejes and K.J. Johnson, "Ohmic contact penetration and encroachment in GaAs/AlGasAs and GaAs FET's," *IEEE Trans. Electron Devices*, Vol. 36, No. 2, pp. 281-288, 1989.

[11] W.P. Hong, K.S. Seo, P.K. Bhattacharya and H. Lee, "Low-resistance ohmic contacts to AlGaAs/GaAs and $In_{0.52}Al_{0.48}As/In_{0.53}Ga_{0.47}As$ modulation-doped structures obtained by halogen lamp annealing," *IEEE Electron Device Lett.*, Vol. 7, pp. 320-323, 1966.

[12] C.K Reeves and H.B. Harrison, "Obtaining the specific contact resistance from transmission line model measurements," *IEEE Electron Device Lett.*, Vol. EDL-3, No. 5, pp. 111-113, 1982.

[13] F. Vidimari, "Improved ohmic properties of Au-Ge contacts to thin *n*-GaAs layers alloyed with an $SiO_2$ overlayer," *Electron. Lett.*, Vol. 15, No. 21, pp. 674-676, 1979.

[14] K. Heime, U. Konig, E. Kohn and A. Wortmann, "Very low resistance Ni-AuGe-Ni contacts to ${}_n$-GaAs," *Solid-State Electron.*, Vol. 17, pp. 835-837, 1974.

[15] R.E. Williams, *Gallium Arsenide Processing Techniques*, Artech House, Boston, p. 236, 1984.

[16] W.D. Edwards, W.A. Hartman and A.B. Torrens, "Specific contact resistance of ohmic contacts to gallium arsenide," *Solid-State Electron.*, Vol. 15, pp. 387-392, 1972.

[17] G.Y. Robinson, "Metallurgical and electrical properties of alloyed Ni/Au-Ge films on n-type GasAs," *Solid-State Electron.*, Vol. 18, pp. 331-342, 1975.

[18] A. Callegani, E.T-S. Pan and M. Murakami, "Uniform and thermally stable AuGeNi ohmic contacts to GaAs," *Appl. Phys. Lett.*, Vol. 46, No. 12, pp.1141-1143, 1985.

[19] Y.C. Shih, M. Murakami, W.H. Price, E.L. Wilkie and A.C. Callegani, "Effects of interfacial microstructure on uniformity and thermal stability of AuNiGe ohmic contact to *n*-type GaAs," *J. Appl. Phys.*, Vol. 62, No. 2, p. 582-590, 1997.

[20] M. Murakami, K.D. Childs, J.M. Baker and A. Callegani, "Microstructure studies of AuNiGe ohmic contacts to *n*-type GaAs," *J. Vac. Sci. Technol. B4*, pp. 903-911, 1986.

[21] G.S. Sravanan, K.M. Bhat, K. Muraleedharan, H.P. Vyas, R. Muralidharan and A. P. Pathak, "Ohmic contacts to pseudomorphic HEMTs with low contact resistance due to enhanced Ge penetration through the AlGaAs layers," *Semicond. Sci. Technol.*, Vol. 23, pp. 1-6, 2008.

## ACKNOWLEDGEMENTS

The authors would like to thank Sue Harris, Dan Nichols and Debbie Ehlers at Agilent Technologies for producing the FIB-SEM cross section images and Dr. Udit Sharma at Evans Analytical Group for producing the TEM images and associated EDS analyses.

## ACRONYMS

pHEMT: Pseudomorphic High Electron Mobility Transistor
TLM: Transmission Line Method
PECVD: Plasma Enhanced Chemical Vapor Deposition
SEM: Scanning Electron Microscope
FIB: Focused Ion Beam
TEM: Transmission Electron Microscope
EDS: Electron Dispersive Spectroscopy
OC: Ohmic Contact
HAADF: High Angle Annular Dark Field